Density Functional Theory Determination of an Axial Gateway To Explain the Rate and Endo Selectivity Enhancement of Diels−Alder Reactions by Bis(oxazoline)-Cu(II)

Jason DeChancie, Orlando Acevedo, and Jeffrey D. Evanseck*

Contribution from the Center for Computational Sciences and the Department of Chemistry and Biochemistry, Duquesne University, 600 Forbes Avenue, Pittsburgh, Pennsylvania 15282-1530

Received August 1, 2003; E-mail: evanseck@duq.edu

Abstract: A novel conceptual model and unique understanding of rate and endo selectivity enhancements delivered by bis(oxazoline)-Cu(II) Lewis acid catalysts in the Diels−Alder reaction of cyclopentadiene and acrylate imide is presented. Despite previously reported kinetic and spectroscopic studies, the physical reasons for endo selectivity and rate enhancements remain poorly understood. Large-scale density functional calculations using Becke three-parameter density functional theory with the nonlocal correlation of Lee, Yang, and Parr and the 6-31G(d) basis set have been carried out for the first time to understand the geometric and energetic consequences of C_2-substituent variation. The unique positioning of the *tert*-butyl C_2-substituent with respect to the diene, referred to as the "axial gateway", maintains the electrophilicity of the catalyst by shielding the reactive metal center from nucleophilic attack. The interplay between steric and electronic factors is crucial to understanding the observed enhanced rates and endo selectivity.

Introduction

Bis(oxazoline) copper(II) complexes are effective enantioselective Lewis acid catalysts for a wide range of important organic reactions. Specifically, the kinetic and synthetic utility of these catalysts have been well documented for the Diels−Alder reaction.[1,2] C_2-symmetric bis(oxazoline) copper(II) complexes have been shown to impact Diels−Alder reactions that typically involve α,β-unsaturated carbonyl compounds with electron-rich olefins (Scheme 1).[2]

In the use of Lewis acid catalysts, stereoelectronic effects clearly impact the observed enantioselectivity and rate enhancements of many Diels−Alder cycloadditions; however, reactions have been reported which escape such explanation.[1] Alternative interpretations have been formulated, yet a consistent model that explains all of the data has not been presented. It is generally recognized that the subtle interplay between steric and electronic factors is crucial to the development of an accurate mechanistic appreciation of chiral Lewis acid-catalyzed Diels−Alder reactions. Despite extensive efforts, focused upon metal center coordination geometry,[1d−f,2,3] dienophile conformation,[2] C_2-substituents,[4,5] and electronic effects,[2,4] the physical reasons for endo selectivity and rate enhancements for bis(oxazoline) copper(II)-catalyzed Diels−Alder reactions remain elusive.[1g] To address this issue, large-scale density functional calculations have been carried out to understand the geometric and energetic consequences of C_2-substituent variation of bis(oxazoline) copper(II)-catalyzed Diels−Alder reactions.
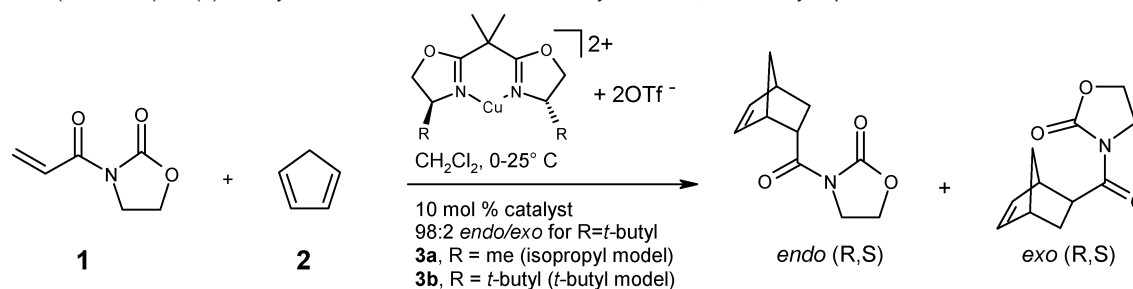
Methods

All density functional calculations were carried out with the Gaussian program,[6] using the computational resources at the Center for Computational Sciences[7] at Duquesne University, Kentucky Superdome, and Pittsburgh Supercomputer Center.[8] Due to limited dispersion forces involving Cu complexes,[9] full geometry optimization and frequency analysis have been carried out using the Becke three-parameter exchange functional[10] with the nonlocal correlation functional of Lee, Yang, and Parr and the 6-31G(d) basis set.[11] UB3LYP/6-31G(d) does not suffer from spin contamination[12] and has been shown to produce realistic structures and energies for pericyclic reactions[13] and [Cu((*S,S*)-Ph-box)]$^{+2}$-catalyzed carbonyl-ene reactions,[14] and reproduce X-ray structures with the phenyl-substituted system.[14] Frequency analysis has been used to confirm all stationary points as minima or transition structures and provide thermodynamic and zero-point energy corrections (Supporting Information). The PCM continuum solvation model is utilized to approximate the effect of solvent by means of single point energy evaluations on the optimized vacuum structures,[15] which has been shown to describe these systems accurately.[14] Contributions due to thermal, vibrational, rotational, and translational motions, including zero-point energies, are included separately by standard statistical mechanical procedures available in Gaussian. The solvent and dielectric constant used is dichloromethane ($\epsilon = 8.93$).

The Mulliken overlap population has been used to gauge the strength of covalent bonding.[16] This indicator is known to be basis set dependent

(1) (a) Evans, D. A.; Johnson, J. S. In *Comprehensive Asymmetric Catalysis*; Jacobsen, E. N., Pfaltz, A., Yamamoto, H., Eds.; Springer: New York, 1999; Vol. 3, 1178−1235 and references therein. (b) Ghosh, A. K.; Mathivanan, P.; Cappiello, J. *Tetrahedron: Asymmetry* **1998**, *9*, 1−45. (c) Jørgensen, K. A. *Angew. Chem., Int. Ed.* **2000**, *39*, 3558−3588. (d) Johnson, J. S.; Evans, D. A. *Acc. Chem. Res.* **2000**, *33*, 325−335. (e) Corey, E. J.; Ishinhara, K. *Tetrahedron Lett.* **1992**, *33*, 6807−6810. (f) Bolm, C.; Martin, M.; Simic, O.; Verrucci, M. *Org. Lett.* **2003**, *5*, 427−429. (g) Rechavi, D.; Lemaire, M. *Chem. Rev.* **2002**, *102*, 3467−3494.
(2) Evans, D. A.; Miller, S. J.; Lectka, T.; von Matt, P. *J. Am. Chem. Soc.* **1999**, *121*, 7559−7573.
(3) (a) Johannsen, M.; Yao, S.; Jørgensen, K. A. *Chem. Commun.* **1997**, *22*, 2169−2170. (b) Johannsen, M.; Jørgensen, K. A. *J. Org. Chem.* **1995**, *60*, 5757−5762.
(4) Evans, D. A.; Johnson, J. S.; Burgey, C. S.; Campos, K. R. *Tetrahedron Lett.* **1999**, *40*, 2879−2882.
(5) Thorhauge, J.; Roberson, M.; Hazell, R. G.; Jørgensen, K. A. *Chem.-Eur. J.* **2002**, *8*, 1888−1898.

Scheme 1. Bis(oxazoline)-Cu(II)-Catalyzed Diels−Alder Reaction of Acrylate Imide, **1**, and Cyclopentadiene, **2**[a]

+ 2OTf[−]

CH₂Cl₂, 0-25° C

10 mol % catalyst
98:2 *endo/exo* for R=*t*-butyl
3a, R = me (isopropyl model)
3b, R = *t*-butyl (*t*-butyl model)

1   **2**

endo (R,S)   *exo* (R,S)

a Catalysts **3a** and **3b** are identical to experiment, minus the *gem*-dimethyl.

and subject to many criticisms. Nevertheless, the Mulliken population overlap has been previously used to understand important secondary orbital interactions.[17−20] To determine the atomic charges, the CHELPG algorithm developed by Breneman and Wiberg has been used.[21] It combines the regular grid of points of Cox and Williams[22] with the Lagrange multiplier method of Chirlian and Francl employed in CHELPG.[23] In CHELPG, a cubic grid of points (spaced 0.3−0.8 Å apart) is used and all grid points that lie within the van der Waals radius of any atom are discarded, together with all points that lie more than 2.8 Å away from any atom. CHELPG charges with 6-31G(d) basis set in all-atom format have been previously shown to be more reliable than the Mulliken charges in solvent simulations.[24]

(6) (a) Frisch, M. J.; Trucks, G. W.; Schlegel, H. B.; Scuseria, G. E.; Robb, M. A.; Cheeseman, J. R.; Zakrzewski, V. G.; Montgomery, J. A., Jr.; Stratmann, R. E.; Burant, J. C.; Dapprich, S.; Millam, J. M.; Daniels, A. D.; Kudin, K. N.; Strain, M. C.; Farkas, O.; Tomasi, J.; Barone, V.; Cossi, M.; Cammi, R.; Mennucci, B.; Pomelli, C.; Adamo, C.; Clifford, S.; Ochterski, J.; Petersson, G. A.; Ayala, P. Y.; Cui, Q.; Morokuma, K.; Malick, D. K.; Rabuck, A. D.; Raghavachari, K.; Foresman, J. B.; Cioslowski, J.; Ortiz, J. V.; Stefanov, B. B.; Liu, G.; Liashenko, A.; Piskorz, P.; Komaromi, I.; Gomperts, R.; Martin, R. L.; Fox, D. J.; Keith, T.; Al-Laham, M. A.; Peng, C. Y.; Nanayakkara, A.; Gonzalez, C.; Challacombe, M.; Gill, P. M. W.; Johnson, B.; Chen, W.; Wong, M. W.; Andres, J. L.; Gonzalez, C.; Head-Gordon, M.; Replogle, E. S.; Pople, J. A. *Gaussian 98*, revision A.3; Gaussian, Inc.: Pittsburgh, PA, 1998. (b) Frisch, M. J.; Trucks, G. W.; Schlegel, H. B.; Scuseria, G. E.; Robb, M. A.; Cheeseman, J. R.; Montgomery, J. A., Jr.; Vreven, T.; Kudin, K. N.; Burant, J. C.; Millam, J. M.; Iyengar, S. S.; Tomasi, J.; Barone, V.; Mennucci, B.; Cossi, M.; Scalmani, G.; Rega, N.; Petersson, G. A.; Nakatsuji, H.; Hada, M.; Ehara, M.; Toyota, K.; Fukuda, R.; Hasegawa, J.; Ishida, M.; Nakajima, T.; Honda, Y.; Kitao, O.; Nakai, H.; Klene, M.; Li, X.; Knox, J. E.; Hratchian, H. P.; Cross, J. B.; Adamo, C.; Jaramillo, J.; Gomperts, R.; Stratmann, R. E.; Yazyev, O.; Austin, A. J.; Cammi, R.; Pomelli, C.; Ochterski, J. W.; Ayala, P. Y.; Morokuma, K.; Voth, G. A.; Salvador, P.; Dannenberg, J. J.; Zakrzewski, V. G.; Dapprich, S.; Daniels, A. D.; Strain, M. C.; Farkas, O.; Malick, D. K.; Rabuck, A. D.; Raghavachari, K.; Foresman, J. B.; Ortiz, J. V.; Cui, Q.; Baboul, A. G.; Clifford, S.; Cioslowski, J.; Stefanov, B. B.; Liu, G.; Liashenko, A.; Piskorz, P.; Komaromi, I.; Martin, R. L.; Fox, D. J.; Keith, T.; Al-Laham, M. A.; Peng, C. Y.; Nanayakkara, A.; Challacombe, M.; Gill, P. M. W.; Johnson, B.; Chen, W.; Wong, M. W.; Gonzalez, C.; Pople, J. A. *Gaussian 03*, revision B.03; Gaussian, Inc.: Pittsburgh, PA, 2003.
(7) Center for Computational Sciences (CCS) at Duquesne University is equipped with 32 and 16 processor SGI Altix 3700 and Altix 350 machines, 16 processor IBM SP, and two 16 processor Alpha clusters. See http://vidar.chemistry.duq.edu/ccs.htm.
(8) National Science Foundation grant: AAB/PSC CHE-030008P.
(9) Urban, M.; Sadlej, A. J. *J. Chem. Phys.* **2000**, *112*, 5−8.
(10) Becke, A. D. *J. Chem. Phys.* **1993**, *98*, 5648−5652.
(11) Lee, C.; Yang, W.; Parr, R. G. *Phys. Rev.* **1988**, *37*, 785−789.
(12) Grafenstein, J.; Cremer, D. *Mol. Phys.* **2001**, *99*, 981−989.
(13) Wiest, O.; Montiel, D. C.; Houk, K. N. *J. Phys. Chem. A* **1997**, *101*, 8378−8388.
(14) Morao, I.; McNamara, J. P.; Hillier, I. H. *J. Am. Chem. Soc.* **2003**, *125*, 628−629.
(15) (a) Tomasi, J.; Persico, M. *Chem. Rev.* **1994**, *94*, 2027−2094. (b) Cances, M. T.; Mennucci, B.; Tomasi, J. *J. Chem. Phys.* **1997**, *107*, 3032−3041.
(16) (a) Mulliken, R. S. *J. Chem. Phys.* **1955**, *23*, 1833−1840. (b) Davidson, E. R. *J. Chem. Phys.* **1967**, *46*, 3320−3324.
(17) Singleton, D. A. *J. Am. Chem. Soc.* **1992**, *114*, 6563−6564.
(18) Birney, D. M.; Houk, K. N. *J. Am. Chem. Soc.* **1990**, *112*, 4127−4133.
(19) Alston, P. V.; Ottenbrite, R. M.; Cohen, T. *J. Org. Chem.* **1978**, *43*, 1864−1867.
(20) Salem, L. *J. Am. Chem. Soc.* **1968**, *90*, 543−552.
(21) Breneman, C. M.; Wiberg, K. B. *J. Comput. Chem.* **1990**, *11*, 361−373.
(22) Cox, S. R.; Williams, D. E. *J. Comput. Chem.* **1981**, *2*, 304−323.
(23) Chirlian, L. E.; Francl, M. M. *J. Comput. Chem.* **1987**, *8*, 894−905.

Using the QUIVER program,[25] kinetic isotope effects (KIEs) were calculated and scaled to the B3LYP/6-31G(d) level of theory using the same procedure described by Singleton and Houk.[26,27] The QUIVER program employs the Bigeleisen and Meyer formulation,[28] based on statistical mechanics and classical transition state theory.[29]

Results and Discussion

Four concerted asynchronous pathways are possible for the Diels−Alder reaction of **1** and **2**. The **3a** (methyl) model was chosen for the isopropyl substituent, due to the lack of steric interactions based upon the reported X-ray structure of the isopropyl system, where the isopropyl hydrogen orients toward the catalyst and the methyl groups point harmlessly away. The **3b** (*tert*-butyl) model was used in its entirety to model key steric interactions provided by the *tert*-butyl group. The transition structures are denoted NC (endo s-cis), XC (exo s-cis), NT (endo s-trans), and XT (exo s-trans). Stereospecific NC and XC transition structures for the concerted asynchronous **3a**- and **3b**-catalyzed Diels−Alder reactions are shown in Figures 1 and 2, respectively. The computed activation energies for the s-cis dienophile conformation are favored over s-trans by approximately 5 kcal/mol. Consequently the computed s-trans systems are not discussed (see Supporting Information). The computed results are in excellent agreement with population ratios obtained by lanthanide induced shifts (LIS), which indicate that α,β-unsaturated amides exist predominantly as s-cis.[30]

Secondary kinetic isotope effects (SKIEs) have been calculated to confirm that the computed cycloadditions are concerted and asynchronous[31] (Supporting Information) consistent with other experimental SKIEs for Lewis acid-catalyzed Diels−Alder reactions.[32] For the Diels−Alder reaction between crotonate imide and cyclopentadine catalyzed by **3b**, the rate constant was observed to be 8.3×10^{-3} M²/min at 0 °C in CH₂Cl₂ with OTf⁻ counterions.[2] Using transition-state theory,[33] the corresponding

(24) Carlson, H. A.; Nguyen, T. B.; Orozco, M.; Jorgensen, W. L. *J. Comput. Chem.* **1993**, *14*, 1240−1249.
(25) Saunders, W.; Laidig, K. E.; Wolfsberg, M. *J. Am. Chem. Soc.* **1989**, *111*, 8989−8994.
(26) Singleton, D. A.; Merrigan, S. R.; Beno, B. R.; Houk, K. N. *Tetrahedron Lett.* **1999**, *40*, 5817−5821.
(27) (a) Storer, J. W.; Raimondi, L.; Houk, K. N. *J. Am. Chem. Soc.* **1994**, *116*, 9675−9683. (b) Wiest, O.; Houk, K. N.; Black, K. A.; Thomas, B., IV. *J. Am. Chem. Soc.* **1995**, *117*, 8594−8599.
(28) (a) Bigeleisen, J.; Mayer, M. G. *J. Chem. Phys.* **1947**, *15*, 261−267. (b) Wolfsberg, M.; Hout, R. F.; Hehre, W. *J. Am. Chem. Soc.* **1980**, *102*, 3296−3298.
(29) Glasstone, S.; Laidler, K. J.; Eyring, H. *The Theory of Rate Processes*; McGraw-Hill: New York, 1941.
(30) Montaudo, G.; Librando, V.; Cacamese, S.; Maravigna, P. *J. Am. Chem. Soc.* **1973**, *95*, 6365−6370.
(31) Acevedo, O.; Evanseck, J. D. *Org. Lett.* **2003**, *5*, 649−652.
(32) Singleton, D. A.; Merrigan, S. R.; Beno, B. R.; Houk, K. N. *Tetrahedron Lett.* **1999**, *40*, 5817−5821.
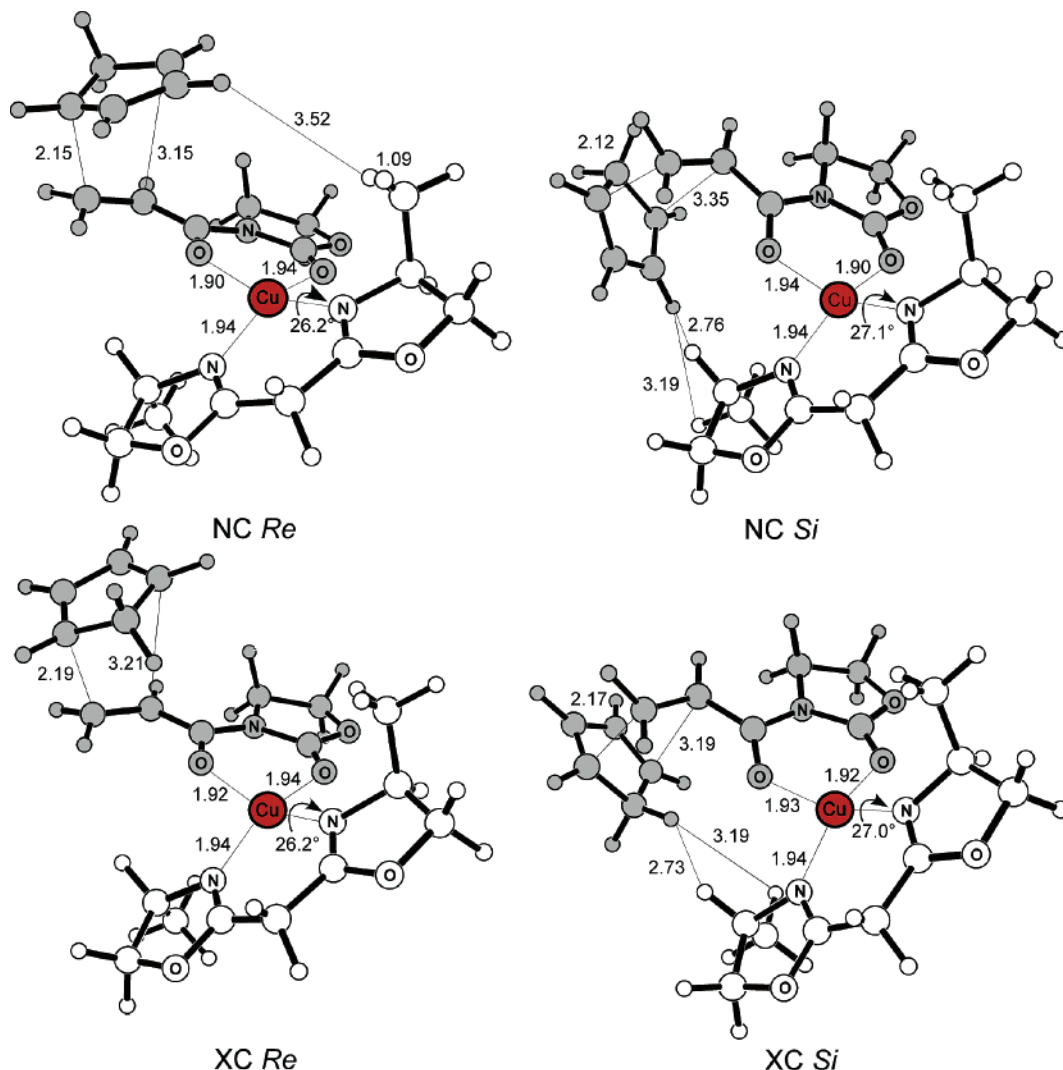
Figure 1. UB3LYP/6-31G(d) optimized transition structures of the **3a**-catalyzed Diels−Alder reaction between **1** and **2**. Bond lengths are reported in angstroms, and dihedral angles are in degrees. The organic reactants are shaded in grey for clarity.

$\Delta G_{273}^{\ddagger}$ is 20.4−20.9 kcal/mol for $\kappa = 0.5$−1.0, respectively. The computed free energy of activation for the **3b**-catalyzed Diels−Alder reaction of **1** and **2** is 19.3 kcal/mol (Table 1), which is in strong agreement with experiment, as described previously.

The computed Gibbs free energy activation barriers of the **3a**-catalyzed system (Table 1) reveal that the Re face approach of the diene is favored. The strongest steric contribution to the NC and XC Si transition structures is the hydrogen directly attached to the carbon bearing the C_2 substituent (Figure 1), which is positioned 2.73 (XC Si) and 2.76 (NC Si) Å from the nearest diene proton. The resulting $\Delta G_{298}^{\ddagger}$ for the NC Si approach is 1 kcal/mol higher in energy than that computed for the corresponding Re system. This steric interaction provides a novel interpretation of facial selectivity, which effectively removes the diene Si face approach independent of the substituent. Therefore, the preferred NC Re pathway has been computed for the **3b**-catalyzed system.

Due to computational limitations, the **3a**-catalyzed system has been used to model solvent effects (Table 1). In a vacuum,

exo selectivity is computed ($\Delta\Delta G_{298}^{\ddagger} = 0.1$ kcal/mol) opposite to that found by experiment for isopropyl, phenyl, and *tert*-butyl systems.[2] However, including solvent (dichloromethane) in the calculations gives endo selectivity, where $\Delta\Delta G_{298}^{\ddagger} = -0.6$ kcal/mol between XC and NC Re. Because facial and endo selectivity is correctly predicted, it is of interest to discover the structural basis of such phenomena.

The computed **3b**-transition structure provides a novel explanation for the enhanced rate and endo selectivity. The enhancements delivered by **3b** can be attributed to the unique positioning of the *tert*-butyl C_2-substituent with respect to the diene, creating an "axial gateway" to the Cu(II) metal center, as shown in Figure 2. One of the methyls from the *tert*-butyl group coupled with one of the endo-diene protons shield the axial approach of nucleophilic attack by creating a steric barrier 2.67 Å wide (closed state), as compared to the larger 3.20 Å distance (open state) for the XC Re **3b** system.[34] For **3a** and **3b**, the solvent-accessible area is tighter for an endo approach due to the constricted axial gateway opening as compared to

(33) Carroll, F. A. *Perspectives on Structure and Mechanism in Organic Chemistry*; Brooks/Cole Publishing Co.: Pacific Grove, 1998; pp 339−342.

(34) Estimated by adding standard methyls onto the optimized XC Re transition structure of **3a**. We find a reasonable agreement between the modified NC Re **3a** distance (2.5 Å) and that of the **3b** system (2.67 Å).
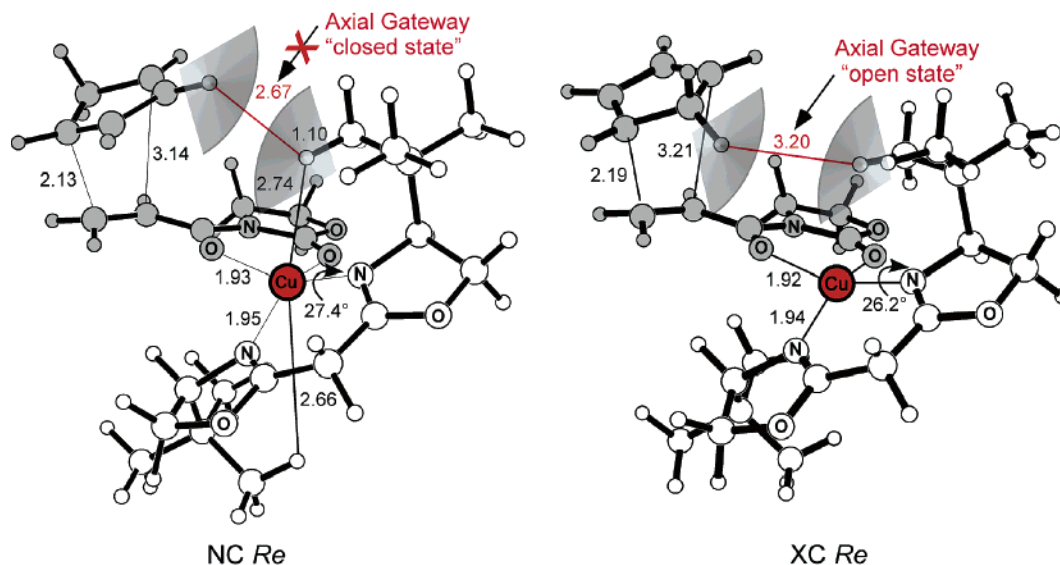
Figure 2. UB3LYP/6-31G(d) optimized transition structure of NC Re and the XC Re transition structure model[34] **3b**-catalyzed Diels−Alder reaction between **1** and **2**. Bond lengths are reported in angstroms, and dihedral angles are in degrees. The organic reactants are shaded in grey for clarity. The axial gateway is illustrated by the constricted space between the grey wedges placed on the diene proton and *t*-butyl hydrogen.

Table 1. UB3LYP/6-31G(d) Activation Energies, Enthalpies, and Gibbs Energies (kcal/mol) for the Reaction of **1** and **2** Catalyzed by **3** in Vacuum and Using PCM Single Points ($\epsilon = 8.93$) on Vacuum Optimized Geometries

			$\Delta E_{298}^{\ddagger}$		$\Delta H_{298}^{\ddagger}$		$\Delta G_{298}^{\ddagger}$	
TS	cat.	face	vacuum	solution	vacuum	solution	vacuum	solution
NC	**3a**	Re	−4.5	7.1	−5.1	6.5	7.8	19.6
NC	**3a**	Si	−3.1	8.3	−3.7	7.8	9.4	20.6
XC	**3a**	Re	−4.4	8.2	−5.0	7.6	7.7	20.2
XC	**3a**	Si	−3.4	8.1	−4.0	7.5	8.9	20.4
NC	**3b**	Re	−3.1	6.1	−3.7	5.5	10.1	19.3[a]

[a] Experimental $\Delta G_{273}^{\ddagger} = 20.4−20.9$ kcal/mol for $\kappa = 0.5−1.0$, respectively, for the Diels−Alder reaction of crotonate, cyclopentadiene, and **3b**.[2]

exo. Thus, Cu(II) is more prone to nucleophilic attack in the exo approach, which as discussed below promotes endo selectivity.

Shielding of the Cu(II) center is necessary to maintain **3b** electrophilicity. We compute that the NC Re *tert*-butyl hydrogen 1s orbital aligns with the Cu(II) $3d_{z^2}$ orbital, yielding a distance of 2.66 and 2.74 Å and an H−Cu−H angle of 155° (Figure 2). As expected for square planar and distorted square planar Cu(II) systems, the axial approach to the copper center is highly electrophilic. The *tert*-butyl C−H bond oriented along the Cu(II) $3d_{z^2}$ orbital axis elongates from 1.09 Å in the unperturbed **3a** system to 1.10 Å in **3b**, signifying the electrophilic power of Cu(II). Most importantly, at a separation distance of 2.74 Å between the copper center and C−H hydrogen, a computed bond elongation of 0.01 Å demonstrates Cu(II)'s ability to function as a strong Lewis acid. For example, when using the same level of theory to describe the C_{2v} lithium cation and water nonbonded complex, a computed O−H bond elongation of only 0.0006 Å results at a distance of 2.23 Å between the lithium cation and water hydrogen. Electron population in the **3b** HOMO increases in the d_{z^2} orbital by 0.029 and decreases for the in-plane Cu(II) d-orbitals by 0.094 as compared to **3a** NC Re. As electron density is drawn to the d_{z^2} orbital, electron density is siphoned from the in-plane d-orbitals. Consequently, shielding of the Cu(II) center from either solvent or nucleophilic counterions

renders it a more powerful catalyst by withdrawing electron density from the dienophile and activating it.

The computations introduce an intriguing question on how counterions impact the structure and reactivity of bis(oxazoline) systems. Counterion effects are known to contribute greatly to the rate and endo selectivity of this Diels−Alder reaction.[2] SbF_6^-, a relatively large ion, increases the catalytic activity, yet decreases endo selectivity, where an opposite effect is demonstrated for the smaller OTf⁻ counterion. The X-ray structure shows that SbF_6^- does not coordinate to the Cu(II) center having distances up to 3.50 Å from the Cu(II) center, because its larger size cannot penetrate through the axial gateway for either NC or XC Re. However, we postulate that the OTf⁻ anion is too large to pass the axial gateway of NC Re, yet small enough to slip through and add to the Cu(II) center, forming a square pyramidal complex for XC Re.[2] Because the newly created covalent bond donates electron density into the catalyst, it diminishes the catalyst's ability to withdraw electron density from the dienophile.[35] This is the origin of the observed retarding effect on the rate when using OTf⁻ as the counterion. In turn, the square pyramidal coordination for XC Re further enhances the endo selectivity by adding more steric congestion, disfavoring exo addition. This conceptual model holds for other reported substituents, where [Cu((*S,S*)-Ph-box)](X₂) cannot shield the Cu-(II) center as effectively and [Cu((*S,S*)-*i*-Pr-box)](X₂) shields only two-thirds of the time, consistent with experimental data.[2]

Summary

The effects of Lewis acidity have been well established for bis(oxazoline) systems, and the influence of counterions has been previously reported. However, the interplay between steric exclusion of solvent and counterions and the direct electronic impact on Lewis acidity at the Cu(II) center is shown here for the first time. The unique positioning of the *tert*-butyl C_2-substituent with respect to the diene at the transition structure creates a steric barrier (called the axial gateway) preventing

(35) Fringuelli, F.; Piermatti, O.; Pizzo, F.; Vaccaro, L. *Eur. J. Org. Chem.* **2001**, 439−455.

nucleophilic attack of the Cu(II) center to maintain its electo-phility and activation of the dieneophile. As such, this study provides an advance in the knowledge of asymmetric reactions and allows for further ideas and development in this exciting area of bis(oxazoline)-Cu(II) catalytic chemistry.

Supporting Information Available: Energies, frequencies, coordinates, and QUIVER outputs of all structures. This material is available free of charge via the Internet at http://pubs.acs.org.

JA037702J